



# Quasiperiodic emissions observed by the Cluster spacecraft and their association with ULF magnetic pulsations

F Němec, O Santolík, J.S. Pickett, Michel Parrot, Nicole Cornilleau-Wehrlin

## ► To cite this version:

F Němec, O Santolík, J.S. Pickett, Michel Parrot, Nicole Cornilleau-Wehrlin. Quasiperiodic emissions observed by the Cluster spacecraft and their association with ULF magnetic pulsations. *Journal of Geophysical Research Space Physics*, 2013, 118, pp.4210-4220. 10.1002/jgra.50406 . insu-01179006

**HAL Id: insu-01179006**

**<https://hal-insu.archives-ouvertes.fr/insu-01179006>**

Submitted on 21 Jul 2015

**HAL** is a multi-disciplinary open access archive for the deposit and dissemination of scientific research documents, whether they are published or not. The documents may come from teaching and research institutions in France or abroad, or from public or private research centers.

L'archive ouverte pluridisciplinaire **HAL**, est destinée au dépôt et à la diffusion de documents scientifiques de niveau recherche, publiés ou non, émanant des établissements d'enseignement et de recherche français ou étrangers, des laboratoires publics ou privés.

# Quasiperiodic emissions observed by the Cluster spacecraft and their association with ULF magnetic pulsations

F. Němec,<sup>1</sup> O. Santolík,<sup>1,2</sup> J. S. Pickett,<sup>3</sup> M. Parrot,<sup>4</sup> and N. Cornilleau-Wehrlin<sup>5,6</sup>

Received 12 March 2013; revised 27 May 2013; accepted 17 June 2013; published 19 July 2013.

[1] Quasiperiodic (QP) emissions are electromagnetic waves at frequencies of about 0.5–4 kHz characterized by a periodic time modulation of the wave intensity, with a typical modulation period on the order of minutes. We present results of a survey of QP emissions observed by the Wide-Band Data (WBD) instruments on board the Cluster spacecraft. All WBD data measured in the appropriate frequency range during the first 10 years of operation (2001–2010) at radial distances lower than  $10 R_E$  were visually inspected for the presence of QP emissions, resulting in 21 positively identified events. These are systematically analyzed, and their frequency ranges and modulation periods are determined. Moreover, a detailed wave analysis has been done for the events that were strong enough to be seen in low-resolution Spatio-Temporal Analysis of Field Fluctuations-Spectrum Analyzer data. Wave vectors are found to be nearly field-aligned in the equatorial region, but they become oblique at larger geomagnetic latitudes. This is consistent with a hypothesis of unducted propagation. ULF magnetic field pulsations were detected at the same time as QP emissions in 4 out of the 21 events. They were polarized in the plane perpendicular to the ambient magnetic field, and their frequencies roughly corresponded to the modulation period of the QP events.

**Citation:** Němec, F., O. Santolík, J. S. Pickett, M. Parrot, and N. Cornilleau-Wehrlin (2013), Quasiperiodic emissions observed by the Cluster spacecraft and their association with ULF magnetic pulsations, *J. Geophys. Res. Space Physics*, 118, 4210–4220, doi:10.1002/jgra.50406.

## 1. Introduction

[2] Whistler mode electromagnetic emissions observed in the magnetosphere at frequencies of about 0.5–4 kHz sometimes exhibit a periodic time modulation of wave intensity. The events with modulation periods of about 4–6 s originating due to ducted whistler mode waves echoing along geomagnetic field-aligned paths between opposite hemispheres, usually called “periodic” emissions, will not be considered in the present study. “Quasiperiodic” (QP) events that we consider have modulation periods greater than 10 s [Helliwell, 1965; Carson *et al.*, 1965; Sazhin and Hayakawa, 1994; Smith *et al.*, 1998] and appear to be mostly a dayside

phenomenon [Ho, 1973; Kimura, 1974; Morrison *et al.*, 1994; Engebretson *et al.*, 2004]. Using the ground-based measurements of magnetic field, they can be further classified as QP emissions type 1 and QP emissions type 2, depending, respectively, on whether or not correlated coincident ULF geomagnetic pulsations are detected [Kitamura *et al.*, 1969; Sato *et al.*, 1974].

[3] QP events of type 1 are closely correlated with coincident geomagnetic pulsations. Quasiperiodic modulations of resonant conditions of wave growth in the wave generation region, governed by compressional ULF magnetic field oscillations, were suggested as their possible generation mechanism [Kimura, 1974; Chen, 1974; Sato and Fukunishi, 1981; Sazhin, 1987; Watt *et al.*, 2011]. This modulation is possible, as already small variations of the magnetic field strength can cause significant variations of the wave growth rate [Coroniti and Kennel, 1970; Kimura, 1974]. The generation region is likely to be located in the outer magnetosphere close to the equatorial plane [Sato and Kokubun, 1980; Sato and Fukunishi, 1981; Morrison, 1990]. A possible importance of high-latitude (nonequatorial) magnetic field minima near the magnetopause for the frequency spectra of the observed QP emissions was considered by Alford *et al.* [1996]. Although most observations of QP emissions are ground-based, spacecraft observations are crucial for understanding their generation mechanisms and propagation properties. This was well demonstrated by Tixier and Cornilleau-Wehrlin [1986], who have shown that the

<sup>1</sup>Faculty of Mathematics and Physics, Charles University in Prague, Prague, Czech Republic.

<sup>2</sup>Institute of Atmospheric Physics, Academy of Sciences of the Czech Republic, Prague, Czech Republic.

<sup>3</sup>Department of Physics and Astronomy, University of Iowa, Iowa City, Iowa, USA.

<sup>4</sup>Laboratoire de Physique et Chimie de l'Environnement et de l'Espace, Centre National de la Recherche Scientifique, Orléans, France.

<sup>5</sup>Laboratoire de Physique des Plasmas, Ecole Polytechnique, CNRS, Palaiseau, France.

<sup>6</sup>LESIA, Observatoire de Meudon, Meudon, France.

Corresponding author: F. Němec, Faculty of Mathematics and Physics, Charles University in Prague, Prague, Czech Republic. (frantisek.nemec@gmail.com)

classification between QP emissions of type 1 and type 2 is not so obvious in the space observations as on the ground, suggesting that both types of QP emissions might have the same generation mechanism. *Pasmanik et al.* [2004] presented a few cases of QP emissions detected on board the Freja and the Magion 5 satellites, along with possible scenarios for their formation. *Hayosh et al.* [2013] reported on three events with simultaneous periodic modulation of VLF wave intensity and energetic electron precipitation found in the low-altitude Detection of Electro-Magnetic Emissions Transmitted from Earthquake Regions (DEMETER) satellite data. *Němec et al.* [2013] presented a case study of a large-scale long-lasting QP event observed simultaneously on board the DEMETER and the Cluster spacecraft and demonstrated that the same QP modulation of the wave intensity is observed at the same time at very different locations in the inner magnetosphere.

[4] Precipitating electron fluxes should exhibit quasiperiodic pulsations as a result of the QP generation process [Coroniti and Kennel, 1970], which was observed by *Gendrin et al.* [1970a, 1970b]. These quasiperiodic modulations of precipitating electron fluxes can subsequently generate quasiperiodic magnetic pulsations in the ionosphere [Bell, 1976; Sato and Kukubun, 1981; Sato and Matsudo, 1986], which can be observed on the ground and explain some of the observed magnetic field fluctuations related to QP emissions [Sato and Fukunishi, 1981]. It is thus of a significant importance to analyze the properties of QP emissions and coincident ULF magnetic field oscillations in situ, close to the generation region.

[5] We present a survey of QP emissions observed by the WBD instruments on board the Cluster spacecraft during the first 10 years (2001–2010) of the mission. Since Cluster is a multispacecraft mission, sampling a large range of radial distances and periodically crossing the geomagnetic equator, it is ideally suited for observations of QP emissions in/close to their probable source region. Moreover, multicomponent measurements of the electromagnetic field obtained by the Spatio-Temporal Analysis of Field Fluctuations-Spectrum Analyzer (STAFF-SA) instruments allow us to perform a detailed wave analysis, and the fluxgate magnetometers (FGM) instruments measuring the three components of the magnetic field are well suited for detection of a possible correlation with ULF magnetic field pulsations. Section 2 describes the data set used in the study. The obtained results are presented in section 3 and discussed in section 4. Finally, section 5 contains a brief summary.

## 2. Data Set

[6] Cluster is a project of the European Space Agency (ESA), which consists of four spacecraft that move in a close formation along an elliptical orbit with a perigee of about 24,000 km, and an apogee of about 119,000 km (the spacecraft orbit slightly changed over the duration of the mission). The data used in the presented study were obtained by the Wide-Band Data (WBD) Plasma Wave investigation instruments, which were designed to provide high-resolution waveform measurements of both AC electric and magnetic fields [Gurnett et al., 1997]. In the continuous baseband measurement mode which is suitable for this study, the data are band-pass filtered in the frequency range 25 Hz–9.5 kHz

and measured with the sampling frequency of 27,443 Hz. The WBD instruments obtain waveforms of either one electric field component or one magnetic field component. These are periodically cycled, so that the approximately 42 s long measurement of the electric field component in the spin plane of the spacecraft is followed by the approximately 10 s long measurement of one magnetic field component, and then the whole pattern is repeated again. Due to the high telemetry rate and the need for ground stations to receive the WBD data directly from the spacecraft, the WBD instruments obtain data over only approximately 4% of the orbit and are thus active only during specifically selected time intervals.

[7] In addition to these high-resolution, one-component measurements, multicomponent wave measurements are performed by the onboard Spectrum Analyzer of the STAFF experiments, STAFF-SA [Cornilleau-Wehrin et al., 1997, 2003]. STAFF-SA calculates the elements of the  $5 \times 5$  complex spectral matrices, from the three orthogonal magnetic field components and the two electric field components in the spin plane. The analysis on board is limited to 27 logarithmically spaced frequency channels between 8 Hz and 4 kHz, and there is one matrix per frequency channel and time interval. This permits to get information about power spectral densities, mutual phases, and coherence relations that can be used to determine detailed wave properties [see, e.g., Santolik et al., 2003, and references therein]. Finally, the Cluster spacecraft are equipped with fluxgate magnetometers (FGM) that provide us with measurements of three components of the ambient magnetic field [Balogh et al., 1997, 2001]. The time resolution varies depending on the mode of the instrument, being equal to 0.2 s in the normal measurement mode.

[8] We have visually inspected all the WBD Survey Plots (<http://www-pw.physics.uiowa.edu/plasma-wave/istp/cluster/mop/>) corresponding to the data measured at radial distances lower than  $10 R_E$  during the first 10 years of operation (2001–2010) for the presence of QP emissions. Altogether, the plots corresponding to about 150 days of WBD data have been analyzed. These cover all magnetic local times (MLTs), all magnetic latitudes, and all  $L$ -shells greater than about 4. All the plots were resized so that a frequency-time spectrogram corresponding to the frequency interval from 0 to about 13.7 kHz and the time interval of 10 min was plotted on a computer screen at a time. Taking into account typical modulation periods of QP emissions, this length of the plotted time interval proved to be a good choice, as several QP elements necessary for the positive identification of an event are expected to be seen in the same plot. Altogether, 21 QP events have been identified in the data. Please note that if a QP structure is observed at the same time by several Cluster spacecraft, it is considered to be a single QP event. The geomagnetic activity at the times when the QP events were observed approximately corresponded to the overall distribution from the years 2001–2010, i.e., there is no clear correlation between the geomagnetic activity and the occurrence of QP events.

[9] An example of one of the identified events is presented in Figure 1, showing a frequency-time spectrogram of power spectral density of electric field fluctuations measured by the WBD instrument on board Cluster 1 on 23 April 2002 between 0255:00 UT and 0315:00 UT. QP emissions

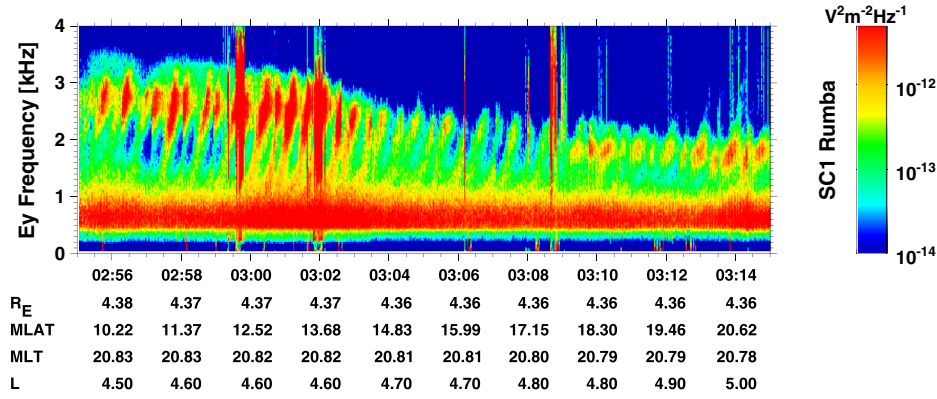


**Figure 1.** Frequency-time spectrogram of power spectral density of electric field fluctuations measured by the WBD instrument on board Cluster 1. QP emissions can be seen at frequencies between about 1 and 3 kHz. The data were measured on 23 April 2002 between 0255:00 UT and 0315:00 UT.

occur at frequencies between about 1 and 3 kHz. Note that cyclic 42 s data intervals of electric field measurements have been dilated across 10 s data intervals where the magnetic field had been measured instead.

### 3. Results

[10] Locations of all the 21 identified QP events are shown in Figure 2. The used coordinates are solar magnetic (SM), so that Figure 2a corresponds to the meridional projection and Figure 2b corresponds to the projection to the equatorial plane. If an event was observed by a single Cluster spacecraft, it is plotted using the black color. If an event was observed simultaneously by several Cluster spacecraft, all the observations are plotted by the same (nonblack) color. Thin black curves in Figure 2a correspond to magnetic field lines with  $L = 2$ ,  $L = 4$ ,  $L = 6$ ,  $L = 8$ , and  $L = 10$ , inner to outer, respectively, calculated using the magnetic dipole model. It can be seen that the events occur over a large range of  $L$ -shells, with most of them being observed within  $45^\circ$  of

the geomagnetic equator at  $L$ -values of about 4 to 6. However, it should be noted that this is likely to be related to the spacecraft sampling, as the Cluster equatorial crossings usually take place at  $L$ -shells slightly larger than 4. Figure 2b demonstrates that the QP events are observed essentially at all magnetic local times.

[11] Beginning and ending frequencies and times of each of the elements forming the QP events have been manually identified for each of the events, which allows us to conveniently analyze their detailed properties. Figure 3 shows a histogram of frequencies of the events. It was constructed in such a way that for each QP event, all corresponding elements were considered, not taking into account by which Cluster spacecraft they were observed. This is justified by the observational fact that if a QP event is detected by more than one Cluster spacecraft at about the same time, the frequency ranges observed by individual spacecraft are about the same. For each QP event, and for each 1 Hz-wide frequency bin in the frequency range of interest, a ratio of QP elements with frequencies contributing to this frequency bin

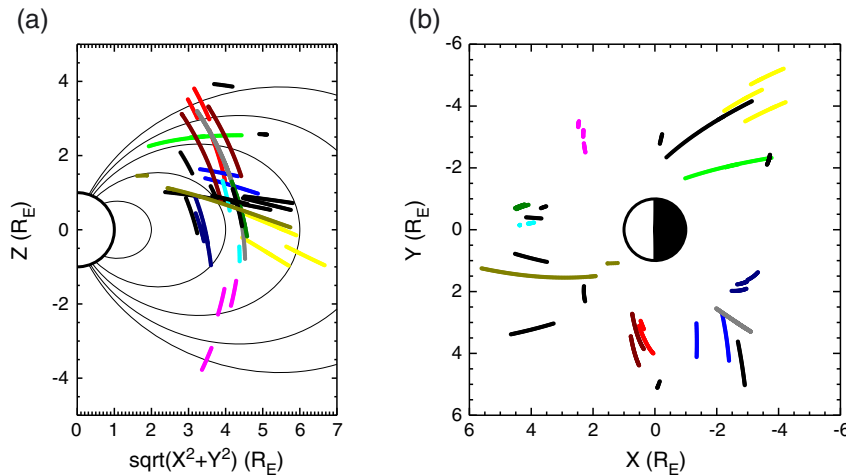


**Figure 2.** Locations of individual QP events in SM coordinates. (a) Meridional view. (b) Equatorial plane view. If an event was observed by a single Cluster spacecraft, it is plotted using the black color. If an event was observed simultaneously by several Cluster spacecraft, all the observations are plotted by the same (nonblack) color. Thin black curves in Figure 2a correspond to magnetic field lines with  $L = 2$ ,  $L = 4$ ,  $L = 6$ ,  $L = 8$ , and  $L = 10$ , inner to outer, respectively, calculated using the magnetic dipole model.

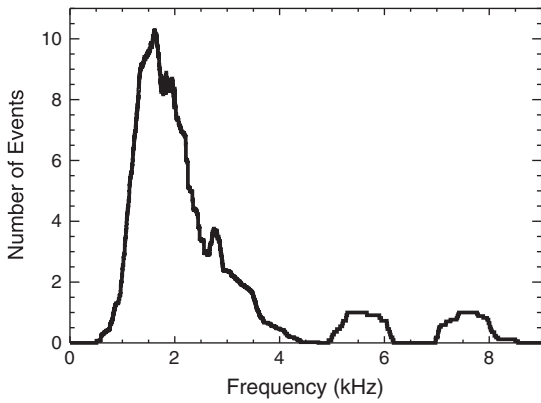


**Figure 3.** Histogram of frequencies of QP events (see text).

has been evaluated. Finally, the values obtained for each frequency bin have been summed over all QP events. It can be seen that the events occur mostly at frequencies from about 1 to 4 kHz, but they can be occasionally observed at frequencies as high as 8 kHz.

[12] The time separation between the individual elements forming QP events, i.e., the modulation period, is not a function of the frequency. It is thus sufficient to determine the modulation period of an event at one chosen frequency. We have chosen this frequency to correspond to the central frequency of a given QP event. This is defined as an arithmetic average of a median of minimum frequencies of individual QP elements and a median of maximum frequencies of individual QP elements. The modulation period has been then determined for each of the events, and for each Cluster spacecraft that observed it, as a median of time separations between consecutive QP elements. It should be noted that the time separation between consecutive QP elements can vary over the time duration of the event [Němec *et al.*, 2013]. However, these variations are typically rather minor, and, given a possible inaccuracy in identifying the QP elements (and possibly even missing some of them), the usage of median was found to be a simple and effective approach of characterizing the modulation period of an event.

[13] The modulation periods have been evaluated for all Cluster observations separately. However, it is found that the modulation periods of a single event determined from different Cluster spacecraft (i.e., at different locations, and, possibly, at different times) are approximately equal (not shown). Consequently, if a QP event is observed by more than one Cluster spacecraft, an overall modulation period of the event can be calculated as an arithmetic average of the time modulations observed by individual spacecraft. A histogram of overall modulation periods of the analyzed QP events is shown in Figure 4. Most of the events are found to have low modulation periods ( $< 2$  min), with the number of events decreasing systematically toward larger periods. The minimum modulation period found was equal to about 0.2 min, while the maximum modulation period found was equal to about 6.1 min.

[14] Multicomponent measurements performed by the STAFF-SA instruments on board the Cluster spacecraft allow us to perform a detailed wave analysis of QP emissions, i.e., among others, to determine the wave vector

and Poynting vector directions [see, e.g., Santolík *et al.*, 2003, and references therein]. However, the instruments have rather poor frequency resolution at higher frequencies where QP emissions are observed. Although the overall frequency bandwidth of a QP event may be rather large, individual elements forming the event drift in frequency, i.e., the frequency bandwidth of a QP element at any given time is rather small. Consequently, a QP event needs to be quite strong in order to be observable in the STAFF-SA data. Among the 21 QP events identified in total in the WBD data, only three were found to be intense enough to be observable also in the STAFF-SA data. The example event from Figure 1 is one of them, at least in the beginning of the time interval when it was observed. Figure 5 shows how this event is seen by the STAFF-SA instruments. Exactly, the same frequency-time interval as in Figure 1 is plotted in order to enable an easy comparison. The meaning of the individual panels of Figure 5 is, from the top: frequency-time spectrogram of power spectral density of magnetic field fluctuations, frequency-time spectrogram of power spectral density of electric field fluctuations, frequency-time plot of planarity of magnetic field fluctuations determined by the singular value decomposition (SVD) method of Santolík *et al.* [2003], frequency-time plot of ellipticity of magnetic field fluctuations determined by the SVD method [Santolík *et al.*, 2002, 2003], frequency-time plot of polar angle of the wave vector direction with respect to the ambient magnetic field determined by the SVD decomposition of the magnetic part of the spectral matrix [Santolík *et al.*, 2003], and frequency-time plot of parallel component of the Poynting flux normalized by the standard deviation [Santolík and Parrot, 1998, 1999].

[15] The values of planarity of magnetic field fluctuations in the third panel of the plot may range from 0 to 1. They express how well the assumption of a single plane wave is fulfilled. The values close to 1 correspond to a situation of a single propagating plane wave, while the values close to 0 correspond to a situation when the polarization ellipsoid degenerates into a sphere, i.e., no preferred direction exists and the wave vector direction cannot be determined from the magnetic part of the spectral matrix. Low values of planarity mean that the assumption of a single plane wave is not valid. Consequently, only frequency-time intervals with the values of planarity larger than 0.5 have been used to calculate wave

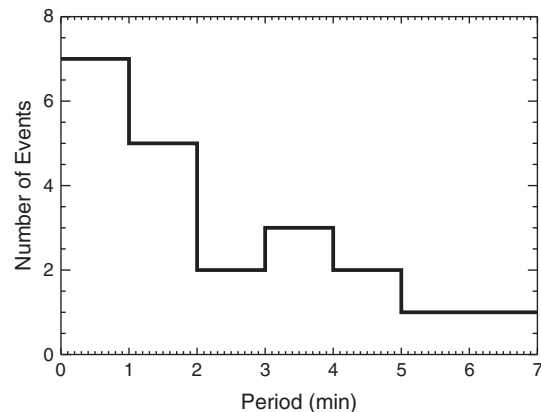


**Figure 4.** Histogram of overall modulation periods of QP events (see text).

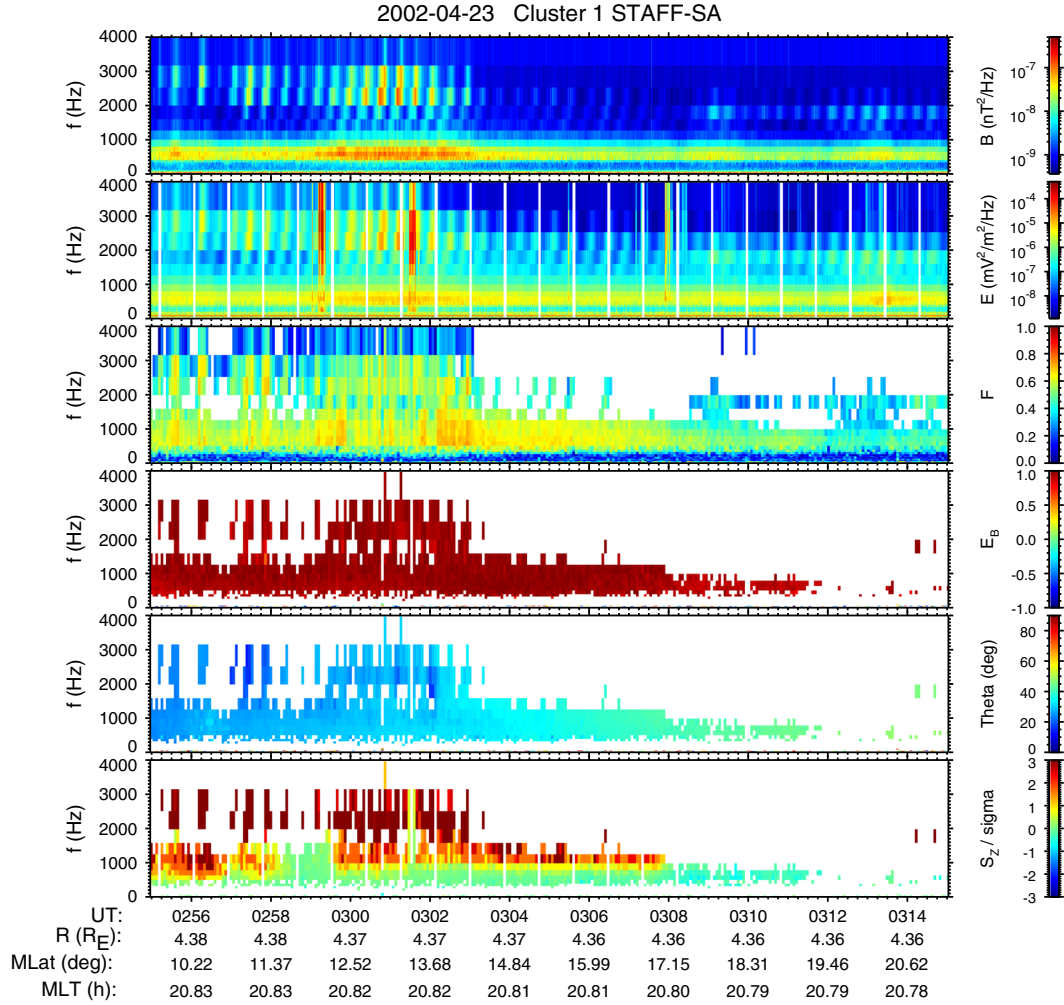


**Figure 5.** Example of a detailed wave analysis using the STAFF-SA instrument. The plotted frequency-time interval is the same as in Figure 1. The meaning of individual panels is (from the top): power spectral density of magnetic field fluctuations, power spectral density of electric field fluctuations, planarity of magnetic field fluctuations determined using the SVD method (see text), ellipticity of magnetic field fluctuations determined using the SVD method (see text), polar angle of the wave vector direction with respect to the ambient magnetic field determined using the SVD method (see text), and parallel component of the Poynting flux normalized by the standard deviation (see text).

and Poynting vector directions. Moreover, only frequency-time intervals with the values of power spectral density of magnetic field fluctuations larger than  $1 \times 10^{-9} \text{ nT}^2 \text{ Hz}^{-1}$  have been considered, since lower power spectral densities of magnetic field fluctuations are considered to be too close to the experimental sensitivity level to give reliable results.

[16] The values of ellipticity of magnetic field fluctuations may range from  $-1$  to  $1$ . The absolute value corresponds to the ratio of the minor to the major polarization axes, and the sign corresponds to the sense of polarization, negative to left-handed and positive to right-handed. It can be seen that the values corresponding to the QP event plotted in the third panel of Figure 5 are close to  $1$ , i.e., the emissions are right-handed nearly circularly polarized. The results obtained for the polar angle of the wave vector direction with respect to the ambient magnetic field are plotted in the fourth panel of Figure 5. Since only magnetic parts of spectral matrices have been used for the calculation, it is not in principle possible to distinguish between two opposite directions of wave

propagation, i.e., there is an ambiguity of  $\pm 180^\circ$ . Values of the polar angle of the wave vector direction may therefore range from  $0^\circ$  to  $90^\circ$ , with  $0^\circ$  corresponding to the wave vector direction along the ambient magnetic field and  $90^\circ$  corresponding to the wave vector direction perpendicular to the ambient magnetic field. It can be seen that for this particular example case, the values are close to  $0^\circ$ , which corresponds to a quasi-parallel propagation of the wave.

[17] The last panel of Figure 5 represents the results obtained for the parallel component of the Poynting flux normalized by its standard deviation, calculated from combined electric and magnetic field measurements. Positive values correspond to the direction along the magnetic field, while negative values correspond to the direction opposite the magnetic field. This effectively solves the unambiguity in wave vector directions determined solely from the magnetic parts of spectral matrices. It can be seen that for this particular example case, the values of the parallel component of the Poynting flux are positive. Taking into account that



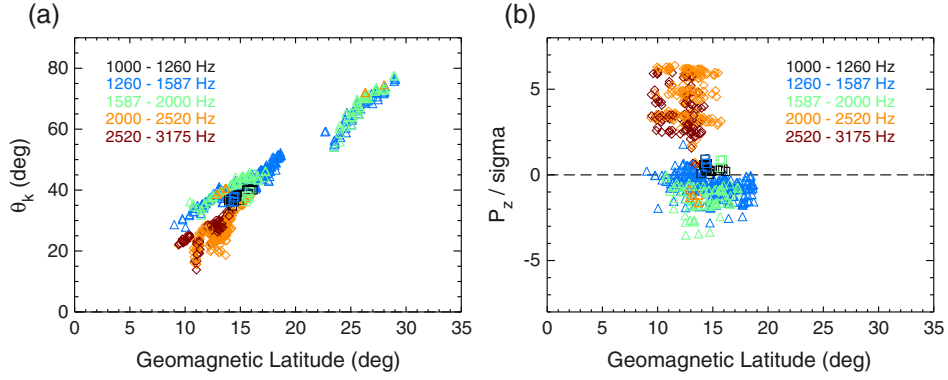


**Figure 6.** (a) Polar angle of the wave vector direction with respect to the ambient magnetic field as a function of the geomagnetic latitude. The wave analysis was done for three different QP events (23 April 2002 02:55–03:15, 01 January 2010 13:40–14:15, and 13 April 2010 08:10–08:40). The results obtained for each of them are plotted by a different symbol (diamond, triangle, and square, respectively). The used frequency ranges of the STAFF-SA instruments are color-coded. (b) Parallel component of the Poynting vector direction normalized by the standard deviation as a function of the geomagnetic latitude. Again, different symbols correspond to different QP events, and different colors correspond to different frequency ranges of the STAFF-SA instruments.

at the time of observation, the spacecraft was located in the Northern Hemisphere, this corresponds to the propagation away from the geomagnetic equator.

[18] The same analysis as for the example case was done for all the three events that were intense enough to be well analyzed by the STAFF-SA instruments (23 April 2002 02:55–03:15, 01 January 2010 13:40–14:15, and 13 April 2010 08:10–08:40). All the emissions were found to be right-handed nearly circularly polarized. The overall results obtained for the polar angle of the wave vector direction with respect to the ambient magnetic field and the parallel com-

ponent of the Poynting flux are shown in Figures 6a and 6b, respectively. The calculated values are plotted as a function of the geomagnetic latitude of the spacecraft at the time of the observation, as this is expected to be the main controlling parameter. The results obtained for each of the three analyzed events are plotted by a different symbol (diamond, triangle, and square). Moreover, the used frequency ranges of the STAFF-SA instruments are color-coded. It should be noted that for a part of the event observed at higher geomagnetic latitudes, only the polar angle of the wave vector direction was determined. The reason is that there was a

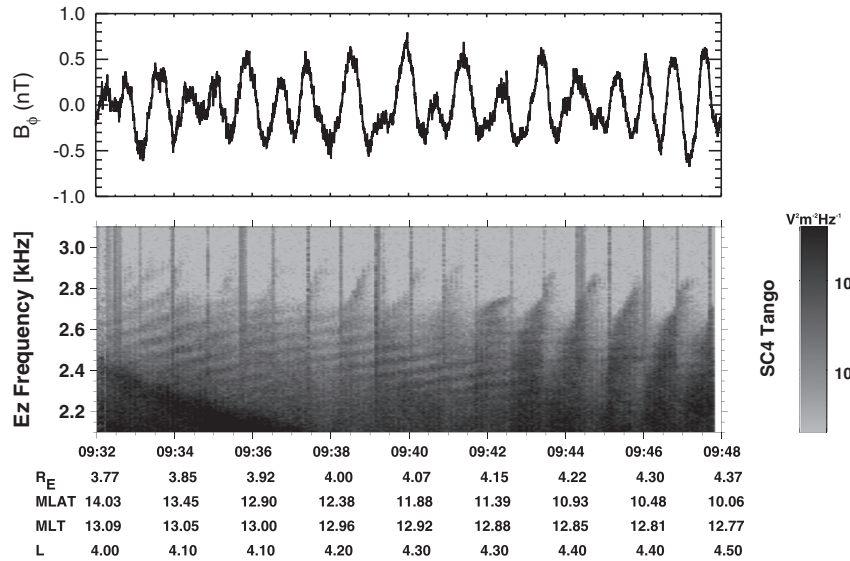


**Figure 7.** (top) ULF magnetic field pulsations measured by the FGM instrument on board Cluster 4 on 22 April 2010 between 0932:00 UT and 0948:00 UT. The plotted amplitude corresponds to the azimuthal direction, with a biquadratic fit subtracted. (bottom) Frequency-time spectrogram of power spectral density of electric field fluctuations measured by the WBD instrument on board Cluster 4 during the same time. The period of magnetic field pulsations is of the same order, but somewhat lower, than the modulation period of QP emissions.

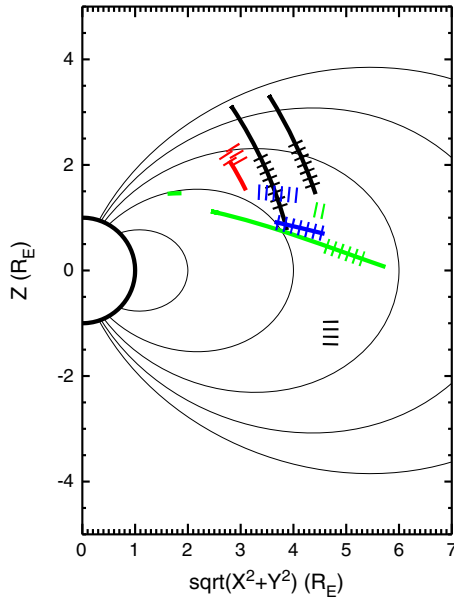


**Figure 8.** (a) Scheme of event locations in SM coordinates for which ULF magnetic field pulsations were observed simultaneously with the QP emissions. Altogether, ULF magnetic field pulsations were detected for four different QP events (11 June 2003 03:47–04:47 [black], 17 December 2006 01:12–01:17 [red], 13 April 2010 07:52–09:07 [green], and 22 April 2010 09:32–09:48 [blue]), the results obtained for each of them being plotted by a different color. The locations where QP electromagnetic emissions were observed are shown by thick solid curves. The locations where ULF magnetic field pulsations were observed are shown by periodic short transverse lines.

temporary problem with electric field measurements performed by Cluster 2, and these are necessary for determining the Poynting vector direction.

[19] Although only three events could be analyzed, it can be seen in Figure 6a that the wave normal angle systematically increases as a function of the geomagnetic latitude. Although the wave vector is quasi-parallel to the magnetic field close to the geomagnetic equator, it becomes more and more oblique at larger geomagnetic latitudes. This shows that QP emissions propagate unducted. The obliqueness of the wave vector means (with an exception of the Gendrin angle) that the group velocity of the emissions is also oblique to the ambient magnetic field. However, the group velocity is generally more field-aligned than the wave vector direction, and its deviation from the magnetic field direction is not expected to exceed about  $20^\circ$ . As for Figure 6b, no clear dependence of the parallel component of the Poynting flux has been found. The waves propagate away from the geomagnetic equator in one event (the example event from Figures 1 and 5). However, the results obtained for the remaining two events are rather inconclusive, indicating a possible propagation both toward and away from the geomagnetic equator.

[20] The fact that the Cluster spacecraft are equipped with fluxgate magnetometers provides us a unique opportunity to check for ULF magnetic field pulsations possibly related to QP emissions. Although this verification has been rather

routinely done on the ground [Kitamura *et al.*, 1969; Sato *et al.*, 1974], spacecraft provide us with a great advantage of being located close to the probable source region of the emissions, i.e., to observe the ongoing phenomena in situ. We have visually inspected all the FGM data measured during the time intervals when the QP emissions were observed for the presence of periodic ULF magnetic field pulsations. Among all the 21 time intervals corresponding to the QP events, we were able to identify the ULF magnetic field pulsations in four of them (11 June 2003 03:47–04:47, 17 December 2006 01:12–01:17, 13 April 2010 07:52–09:07, and 22 April 2010 09:32–09:48).

[21] A QP event with ULF pulsations measured by Cluster 4 on 22 April 2010 between 0932:00 UT and 0948:00 UT is shown in Figure 7. A frequency-time spectrogram of power spectral density of electric field fluctuations corresponding to a QP event measured by the WBD instrument is shown in the bottom panel. Again, cyclic 42 s data intervals of electric field measurements have been dilated across 10 s data intervals where the magnetic field had been measured instead. Moreover, the black-and-white version of the figure is used, as it allows for more contrast and makes the structure more visible. Note that the periodic vertical lines in the figure are a result of an automatic gain adjustment when switching from the magnetic to electric antenna. Also, note that the lines with low frequency drifts observed at lower frequencies correspond to an MLR event [Němec *et al.*, 2012a, 2012b], which is—interestingly enough—observed simultaneously with the QP event, and at the times around 0938:00 UT, the two might appear even related. However, this is a topic for a separate study, and it will not be discussed any further in this paper. The top panel of Figure 7 shows the ULF magnetic field pulsations measured by the FGM instrument at the same time. The plotted amplitude corresponds to the azimuthal direction, which is about the direction of the major polarization axis. Moreover, a biquadratic fit has been subtracted in order to remove the magnetic field variation due to the spacecraft movement. It can be seen that the period of magnetic field pulsations is of the same order as the modulation period of QP emissions, but—in this particular case—by a factor of about 1.7 lower. Another example of simultaneous observations of a QP event and ULF magnetic field pulsations, corresponding to the event from 13 April 2010, was presented by Němec *et al.* [2013] (see their Figure 7).

[22] Locations of all four of the events where QP emissions were observed along with coincident ULF magnetic pulsations are shown in Figure 8. Results obtained for each of the events are plotted by a different color. The example event from Figure 7 is plotted in blue, the event reported by Němec *et al.* [2013] is plotted in green. The locations where QP electromagnetic emissions were observed by the WBD instruments are shown by thick solid curves. The locations where ULF magnetic field pulsations were observed are shown by periodic short transverse lines. Note that even if the WBD instrument was not operating at a given time on a given spacecraft (so that it did not see the QP emissions forming for a given event), ULF magnetic field pulsations may still have been detected by the spacecraft.

[23] It can be seen that the ULF magnetic field pulsations are observed at geomagnetic latitudes up to about  $40^\circ$ . Since all the three components of the magnetic field are measured,



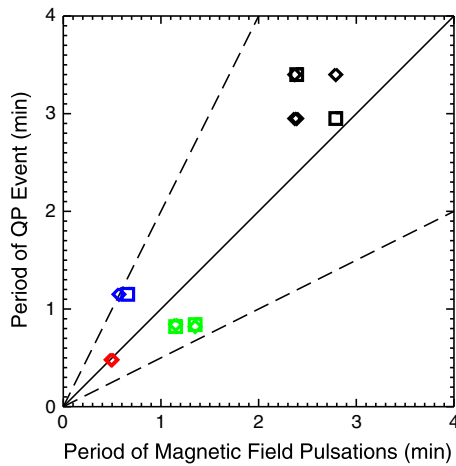


**Figure 9.** Modulation period of QP events as a function of the period of coincident ULF magnetic field pulsations detected by the FGM instrument. The same four events as in Figure 8 are analyzed, and they are again distinguished by different colors. If the ULF magnetic field pulsations were observed by the same Cluster spacecraft as the QP emissions, the appropriate data point is plotted as a square. If the ULF magnetic field pulsations were observed by a different Cluster spacecraft than the QP emissions, the appropriate data point is plotted as a diamond. The solid diagonal line corresponds to the situation of QP modulation period being the same as the period of ULF magnetic field pulsations. The dashed lines correspond to the situation of QP modulation period being equal to the double of the period of ULF magnetic field pulsations, and to the half of the period of ULF magnetic field pulsations, respectively.

the information about the wave polarization can be obtained. It is found that the ULF magnetic field oscillations are generally polarized in the plane perpendicular to the ambient magnetic field (within less than  $20^\circ$  in all cases). Moreover, the major polarization axis of the ULF magnetic field oscillations was oriented in the azimuthal direction. The only exception was the event plotted by green color in Figure 8, for which the ULF magnetic field oscillations were polarized primarily in the radial direction. Magnitudes of the observed ULF magnetic field pulsations are on the order of a few nT.

[24] Having identified the four QP events for which ULF magnetic field pulsations are observed along with the electromagnetic emissions, a natural question arises, viz., what is the relation between their modulation periods. This is answered in Figure 9, which shows the modulation period of QP events as a function of the period of simultaneously detected ULF magnetic field pulsations. The same four events as in Figure 8 are analyzed, and they are again distinguished by colors. Several data points are plotted for each of the events, corresponding to all possible combinations of the spacecraft observing QP emissions and the spacecraft observing ULF magnetic field pulsations. If the ULF magnetic field pulsations were observed by the same Cluster spacecraft as the QP emissions, the appropriate data point is plotted as a square. If the ULF magnetic field pulsations were observed by a different Cluster spacecraft than the QP emissions, the appropriate data point is plotted as a diamond. The solid diagonal line corresponds to the situation of QP

modulation period being the same as the period of ULF magnetic field pulsations. The dashed lines correspond to the situation of QP modulation period being equal to the double of the period of ULF magnetic field pulsations and to the half of the period of ULF magnetic field pulsations, respectively. It can be seen that although the scatter of the data points is rather large, there appears to be—within a factor of 2—a relation between the modulation period of QP events and the period of ULF magnetic field pulsations. For two events (red, black), the two periods are about the same; for one event (blue), the period of ULF magnetic field pulsations is equal to about 0.5–0.6 of the modulation period of the QP event; and for one event (green), the period of ULF magnetic field pulsations is by a factor of about 1.6–1.7 larger than the modulation period of QP emissions. The results are rather independent of whether the QP emissions are observed by the same spacecraft as the ULF magnetic field pulsations or not.

#### 4. Discussion

[25] The presented systematic study of QP emissions observed by the WBD instruments on board the Cluster spacecraft uses multipoint high-resolution wave data measured over a large range of radial distances along spacecraft orbits periodically sampling the equatorial region, which is likely to be the source region of QP emissions [Sato and Kokubun, 1980; Sato and Fukunishi, 1981; Morrison, 1990]. A detailed wave analysis is possible due to the multicomponent STAFF-SA measurements, and moreover, prospective coincident ULF magnetic field pulsations can be analyzed using the FGM instruments. Consequently, the used data set has some major benefits as compared to the ground-based measurements, which are performed far from the source region, and for which the QP emissions are affected by the propagation in the Earth-ionosphere waveguide [Morrison, 1990; Engebretson *et al.*, 2004] and the ULF magnetic field pulsations are affected by the ionosphere [Bell, 1976; Sato and Kokubun, 1981; Sato and Matsudo, 1986].

[26] On the other hand, the amount of data obtained by the WBD instruments in the region of interest, as well as their coverage, is limited. This, along with only 21 QP events identified in total, prevents us from drawing any firm conclusions concerning the occurrence of QP emissions, either in the sense of preferred geomagnetic conditions or in the sense of preferred  $L$ -shells/MLTs. Nevertheless, Figure 2 shows that QP emissions occur over a large range of  $L$ -shells and that they are observed at nearly all MLTs.

[27] Although the total number of identified QP events is not particularly high, it is sufficient to perform at least a rough analysis of typical frequency ranges and modulation periods (Figures 3 and 4). The observations of the same event by several different Cluster spacecraft provide us with a unique opportunity to analyze the same event at several different points in the space. It is found that the frequency-time features of QP emissions are generally the same at all Cluster spacecraft that observe them, in agreement with the case study results obtained by Němec *et al.* [2013]. Small differences between individual Cluster spacecraft can be—apart from inaccuracies arising from manual selection of QP elements on a computer screen—explained by a time evolution of the event and the fact that the time interval

when a given event is observed may vary from spacecraft to spacecraft.

[28] Frequencies of most of the observed QP events are in the frequency range from about 1 to 4 kHz. However, two events were detected at larger frequencies, demonstrating that QP emissions can occur at frequencies as high as nearly 8 kHz. As for the modulation periods, these are found to be on the order of a couple of minutes, with lower modulation periods occurring more frequently. No clear correlation between the radial distance/ $L$ -shell of observation and the frequency range/modulation period has been found. However, the number of available events is too small to obtain any firm conclusions, especially taking into account that there might be several controlling factors acting simultaneously.

[29] Detailed wave analysis of QP emissions, which is possible due to multicomponent measurements performed by the STAFF-SA instruments, represents a unique opportunity to observe and understand the propagation properties of the waves. Taking into account that some of our observations are made close to the equatorial plane at radial distances of a few Earth radii, i.e., in the probable source region of the emissions, the results of a detailed wave analysis become even more interesting. Unfortunately, the frequency resolution of the STAFF-SA instruments in the frequency range from about 1 to 4 kHz, i.e., in the frequency range typical for QP emissions, is rather poor. Consequently, only strong events with sufficient frequency bandwidth are detected by the STAFF-SA instruments. This limits the analysis of detailed wave properties to only three events. The amount of data is further decreased by the requirement of reasonably large values of power spectral density of magnetic field fluctuations and planarity.

[30] All the analyzed QP event waves were right-handed nearly circularly polarized. The obtained results depicted in Figure 6a show that the wave normal angle increases monotonically as a function of geomagnetic latitude, in agreement with the case study results presented by Němec *et al.* [2013]. This demonstrates that the waves propagate unducted, being quasi-parallel to the ambient magnetic field only close to the geomagnetic equator. Moreover, electric field fluctuations are measured along with magnetic field fluctuations by the STAFF-SA instruments, so that the information about the parallel component of the Poynting vector can be obtained as well (see Figure 6b). Assuming that the waves are generated in the equatorial region, one would expect the wave propagation away from the geomagnetic equator. This was the case for one out of the three analyzed events. The results obtained for the two remaining events are rather inconclusive, but they indicate that QP emissions may propagate toward the geomagnetic equator as well. This suggests a rather complicated propagation pattern of QP emissions.

[31] ULF magnetic field pulsations coincident with QP emissions have been typically reported by using the ground-based magnetometers [Kitamura *et al.*, 1969; Sato *et al.*, 1974]. However, as these are believed to be responsible for the generation of QP emissions, it is of a great importance to measure them in situ, close to the expected generation region. Out of the 21 QP events analyzed in total, ULF magnetic field pulsations were observed by the FGM instruments on board the Cluster spacecraft in four of them. The period of these pulsations corresponded within a factor of 2

to the modulation period of QP emissions (see Figure 9), and their magnitude was on the order of a few nT. They were polarized in the plane perpendicular to the ambient magnetic field in all cases. The major polarization axis in three out of the four cases was oriented in the azimuthal direction. This means that the most likely interpretation of the observed ULF pulsations are standing waves of toroidal mode [Takahashi and McPherron, 1982; Denton *et al.*, 2004]. Moreover, a comparison of theoretically calculated periods [Orr and Matthew, 1971; Schulz, 1996] and the observed periods suggests that they are fundamental mode (odd) standing Alfvén waves. This is consistent with the results of Lanzerotti and Fukunishi [1974], who found that the odd mode is the dominant mode for waves in the period range of about 20 to 200 s near  $L = 4$ . They suggested that the coupling of a driving force to a shear Alfvén wave at the local resonant field line can occur most effectively for the excitation of the odd mode, because it has a maximum displacement at the geomagnetic equator, which we believe may be applicable to our situation. The only event which does not fit into this scheme is the event reported in a case study by Němec *et al.* [2013] (plotted in green in Figures 8 and 9), for which the magnitude of the ULF pulsations was found to be larger at the geomagnetic equator than at higher latitudes, which would favor the even mode. However, as it is the only event where the ULF pulsations are preferentially polarized in the radial direction, and as it was observed very close to the geomagnetic equator, it might be possibly interpreted as an event for which the spacecraft is located close to the place where the driving force (acting in the equatorial plane) excites the standing wave. The absence of ULF pulsations in the remaining 17 QP events can be probably explained by propagation effects: while QP emissions propagate unducted, and they may be therefore observed at  $L$ -shells other than the source region, ULF pulsations are limited to a given interval of  $L$ -shells.

[32] Another important point is to understand whether the detected ULF magnetic field pulsations correspond to the modulating MHD wave responsible for the generation of the QP emissions themselves, or rather to excited standing oscillations of local resonant field lines [Sato and Kukubun, 1981; Tixier and Cornilleau-Wehrin, 1986]. The point is that the mechanisms considered for the generation of QP emissions are generally based on modulation of VLF waves by geomagnetic pulsations, which involve compressional fluctuations of the magnetic field [see, e.g., Kimura, 1974]. However, the observed ULF magnetic field pulsations correspond to shear Alfvén waves rather than to compressional fast magnetosonic waves, i.e., they are not related to the change of the magnetic field magnitude, but rather to the change of the magnetic field direction. Moreover, an exact relation between the period of ULF magnetic field pulsations and the modulation period of QP emissions is rather unclear. Symmetry reasons would indicate that in the case of a shear Alfvén wave, principally, the same situation should occur twice per one ULF oscillation period. This means that if the shear Alfvén waves were responsible for the generation of QP emissions, their period should be twice the period of the resulting QP modulation. In this context, it is of some interest to note that for the event observed closest to the geomagnetic equator (plotted in green in Figures 8 and 9, reported earlier by Němec *et al.* [2013]), the period

of ULF magnetic field pulsations is by a factor of about 1.6–1.7 larger than the modulation period of QP emissions, and moreover, this is the only event polarized primarily in the radial direction. However, in the remaining three events for which ULF magnetic field pulsations were detected, the period of ULF magnetic field pulsations is comparable to the period of QP emissions (two events), or by a factor of nearly 2 lower than the period of QP emissions (one event). This might be possibly linked to a harmonicity of field line oscillations. It seems possible that the compressional ULF magnetic field pulsations responsible for the generation of QP emissions are limited exclusively to a very narrow region close to the geomagnetic equator, so that the spacecraft are not located in the right region to observe them directly, and they observe only excited standing oscillations of local resonant field lines.

## 5. Conclusions

[33] Results of a survey of QP emissions observed by the WBD instruments on board the Cluster spacecraft during the first 10 years of operation (2001–2010) have been presented. Altogether, 21 QP events have been visually identified in the data and analyzed. Whenever possible, high-resolution WBD measurements were complemented by multicomponent STAFF-SA data, and moreover, FGM data have been verified for the presence of simultaneously observed ULF magnetic field pulsations. Observations of QP emissions by several different Cluster spacecraft revealed that when the same event is observed at several different points in the space, its spectral features are generally the same. The emissions were found to occur mostly in the frequency range from about 1 to 4 kHz, but events at frequencies as high as about 8 kHz are possible. Modulation periods of the events were found to be on the order of minutes, with lower periods occurring more frequently. Results of a detailed wave analysis show that while the wave normal angle is nearly field-aligned close to the geomagnetic equator, it monotonically increases at larger geomagnetic latitudes, indicating that the waves propagate unducted. ULF magnetic field pulsations were detected simultaneously with QP emissions in 4 out of 21 events. They were polarized in the plane perpendicular to the ambient magnetic field, and their frequencies roughly corresponded to the modulation period of QP events.

[34] **Acknowledgments.** We would like to thank the Cluster Active Archive and all the involved personnel. We would like to acknowledge E. Lucek, who is the principal investigator of the FGM instrument. A part of the Cluster WBD data set for this study has been received at the Panská Ves Observatory of the Institute of Atmospheric Physics ASCR, and we would like to thank its personnel. This work was supported by GACR grants P209/12/P658 and P205/10/2279. This work was supported at Iowa by NASA Goddard Space Flight Center grant NNX11AB38G.

[35] Robert Lysak thanks Kazue Takahashi and another reviewer for their assistance in evaluating this paper.

## References

Alford, J., M. Engebretson, R. Arnoldy, and U. Inan (1996), Frequency variations of quasi-periodic ELF-VLF emissions: A possible new ground-based diagnostic of the outer high-latitude magnetosphere, *J. Geophys. Res.*, **101**(A1), 83–97.

Balogh, A., et al. (1997), The Cluster magnetic field investigation, *Space Sci. Rev.*, **79**, 65–91.

Balogh, A., et al. (2001), The Cluster magnetic field investigation: An overview of in-flight performance and initial results, *Ann. Geophys.*, **19**, 1207–1217.

Bell, T. F. (1976), ULF wave generation through particle precipitation induced by VLF transmitters, *J. Geophys. Res.*, **81**(19), 3316–3326.

Carson, W. B., J. A. Koch, J. H. Pope, and R. M. Gallet (1965), Long-period very low frequency emission pulsations, *J. Geophys. Res.*, **70**(17), 4293–4303.

Chen, L. (1974), Theory of ULF modulation of VLF emissions, *Geophys. Res. Lett.*, **1**(2), 73–75.

Cornilleau-Wehrin, N., et al. (1997), The Cluster spatio-temporal analysis of field fluctuations STAFF experiment, *Space Sci. Rev.*, **79**(1–2), 107–136, doi:10.1023/A:1004979209565.

Cornilleau-Wehrin, N., et al. (2003), The Cluster spatio-temporal analysis of field fluctuations STAFF experiment, *Ann. Geophys.*, **21**, 437–456.

Coroniti, F. V., and C. F. Kennel (1970), Electron precipitation pulsations, *J. Geophys. Res.*, **75**(7), 1279–1289.

Denton, R. E., K. Takahashi, R. R. Anderson, and M. P. Wuest (2004), Magnetospheric toroidal Alfvén wave harmonics and the field line distribution of mass density, *J. Geophys. Res.*, **109**, A06202, doi:10.1029/2003JA010201.

Engebretson, M. J., J. L. Posch, A. J. Halford, G. A. Shelburne, A. J. Smith, M. Spasojević, U. S. Inan, and R. L. Arnoldy (2004), Latitudinal and seasonal variations of quasiperiodic and periodic VLF emissions in the outer magnetosphere, *J. Geophys. Res.*, **109**, A05216, doi:10.1029/2003JA010335.

Gendrin, R., C. Berthomier, H. Cory, A. Meyer, B. Sukhera, and J. Vigneron (1970a), Very-low-frequency and particle rocket experiment at Kerguelen Islands: 1. Very-low-frequency measurements, *J. Geophys. Res.*, **75**(31), 6153–6168.

Gendrin, R., J. Etcheto, and B. de la Porte des Vaux (1970b), Very-low-frequency and particle rocket experiment at Kerguelen Islands: 2. Particle measurements, *J. Geophys. Res.*, **75**(31), 6169–6181.

Gurnett, D. A., R. L. Huff, and D. L. Kirchner (1997), The wide-band plasma wave investigation, *Space Sci. Rev.*, **79**, 195–208.

Hayosh, M., D. L. Pasmanik, A. G. Demekhov, O. Santolík, M. Parrot, and E. E. Titova (2013), Simultaneous observations of quasi-periodic ELF/VLF wave emissions and electron precipitation by DEMETER satellite. A case study, *J. Geophys. Res. Space Physics*, **118**, doi:10.1002/jgra.50179.

Helliwell, R. A. (1965), *Whistlers and Related Ionospheric Phenomena*, Stanford Univ. Press, CA.

Ho, D. (1973), Interaction between whistlers and quasi-periodic VLF emissions, *J. Geophys. Res.*, **78**(31), 7347–7356.

Kimura, I. (1974), Interrelation between VLF and ULF emissions, *Space Sci. Rev.*, **16**, 389–411.

Kitamura, T., J. A. Jacobs, T. Watanabe, and J. R. B. Flint (1969), An investigation of quasi-periodic VLF emissions, *J. Geophys. Res.*, **74**(24), 5652–5664.

Lanzerotti, L. J., and H. Fukunishi (1974), Modes of magnetohydrodynamic waves in the magnetosphere, *Rev. Geophys.*, **12**(4), 724–729.

Morrison, K. (1990), Quasi-periodic VLF emissions and concurrent magnetic pulsations seen at  $L = 4$ , *Planet. Space Sci.*, **38**(12), 1555–1565.

Morrison, K., M. J. Engebretson, J. R. Beck, J. E. Johnson, R. L. Arnoldy, J. L. J. Cahill, D. L. Carpenter, and M. Gallani (1994), A study of quasi-periodic ELF-VLF emissions at three Antarctic stations: Evidence for off-equatorial generation? *Ann. Geophys.*, **12**, 139–146, doi:10.1007/s00585-994-0139-8.

Němec, F., M. Parrot, and O. Santolík (2012a), Detailed properties of magnetospheric line radiation events observed by the DEMETER spacecraft, *J. Geophys. Res.*, **117**, A05210, doi:10.1029/2012JA017517.

Němec, F., M. Parrot, O. Santolík, and J. S. Pickett (2012b), Magnetospheric line radiation event observed simultaneously on board Cluster 1, Cluster 2 and DEMETER spacecraft, *Geophys. Res. Lett.*, **39**, L18103, doi:10.1029/2012GL053132.

Němec, F., O. Santolík, M. Parrot, J. S. Pickett, M. Hayosh, and N. Cornilleau-Wehrin (2013), Conjugate observations of quasi-periodic emissions by Cluster and DEMETER spacecraft, *J. Geophys. Res. Space Physics*, **118**, 198–208, doi:10.1029/2012JA018380.

Orr, D., and J. A. D. Matthew (1971), The variation of geomagnetic micropulsation periods with latitude and the plasmopause, *Planet. Space Sci.*, **19**, 897–905.

Pasmanik, D. L., E. E. Titova, A. G. Demekhov, V. Y. Trakhtengerts, O. Santolík, F. Jiricek, K. Kudela, and M. Parrot (2004), Quasi-periodic ELF/VLF wave emissions in the Earth's magnetosphere: Comparison of satellite observations and modelling, *Ann. Geophys.*, **22**, 4351–4361.

- Santolík, O., and M. Parrot (1998), Propagation analysis of electromagnetic waves between the helium and proton gyrofrequencies in the low-altitude auroral zone, *J. Geophys. Res.*, **103**(A9), 20,469–20,480.
- Santolík, O., and M. Parrot (1999), Case studies on wave propagation and polarization of ELF emissions observed by Freja around the local proton gyro-frequency, *J. Geophys. Res.*, **104**(A2), 2459–2475.
- Santolík, O., J. S. Pickett, D. A. Gurnett, and L. R. O. Storey (2002), Magnetic component of narrowband ion cyclotron waves in the auroral zone, *J. Geophys. Res.*, **107**(A12), 1444, doi:10.1029/2001JA000146.
- Santolík, O., M. Parrot, and F. Lefeuvre (2003), Singular value decomposition methods for wave propagation analysis, *Radio Sci.*, **38**(1), 1010, doi:10.1029/2000RS002523.
- Sato, N., and H. Fukunishi (1981), Interaction between ELF-VLF emissions and magnetic pulsations: Classification of quasi-periodic ELF-VLF emissions based on frequency-time spectra, *J. Geophys. Res.*, **86**(A1), 19–29.
- Sato, N., and S. Kokubun (1980), Interaction between ELF-VLF emissions and magnetic pulsations: Quasi-periodic ELF-VLF emissions associated with Pc 3–4 magnetic pulsations and their geomagnetic conjugacy, *J. Geophys. Res.*, **85**(A1), 101–113.
- Sato, N., and S. Kokubun (1981), Interaction between ELF-VLF emissions and magnetic pulsations: Regular period ELF-VLF pulsations and their geomagnetic conjugacy, *J. Geophys. Res.*, **86**(A1), 9–18.
- Sato, N., and T. Matsudo (1986), Origin of magnetic pulsations associated with regular period VLF pulsations Type 2 QP observed on the ground at Syowa Station, *J. Geophys. Res.*, **91**(A10), 11,179–11,185.
- Sato, N., K. Hayashi, S. Kokubun, T. Oguti, and H. Fukunishi (1974), Relationships between quasi-periodic VLF emission and geomagnetic pulsation, *J. Atmos. Terr. Phys.*, **36**, 1515–1526.
- Sazhin, S. S. (1987), An analytical model of quasiperiodic ELF-VLF emissions, *Planet. Space Sci.*, **35**(10), 1267–1274.
- Sazhin, S. S., and M. Hayakawa (1994), Periodic and quasiperiodic VLF emissions, *J. Geophys. Res.*, **99**(6), 735–753.
- Schulz, M. (1996), Eigenfrequencies of geomagnetic field lines and implications for plasma-density modeling, *J. Geophys. Res.*, **101**(A8), 17,385–17,397.
- Smith, A. J., M. J. Engebretson, E. M. Klatt, U. S. Inan, R. L. Arnoldy, and H. Fukunishi (1998), Periodic and quasiperiodic ELF/VLF emissions observed by an array of Antarctic stations, *J. Geophys. Res.*, **103**(A10), 23,611–23,622.
- Takahashi, K., and R. L. McPherron (1982), Harmonic structure of Pc 3–4 pulsations, *J. Geophys. Res.*, **87**(A3), 1504–1516.
- Tixier, M., and N. Cornilleau-Wehrin (1986), How are the VLF quasi-periodic emissions controlled by harmonics of field line oscillations? The results of a comparison between ground and GEOS satellites measurements, *J. Geophys. Res.*, **91**(A6), 6899–6919.
- Watt, C. E. J., A. W. Degeling, R. Rankin, K. R. Murphy, I. J. Rae, and H. J. Singer (2011), Ultralow-frequency modulation of whistler-mode wave growth, *J. Geophys. Res.*, **116**, A10209, doi:10.1029/2011JA016730.